BMC Genomics

RESEARCH Open Access

The mitochondrial genome of *Bottapotamon fukienense* (Brachiura: Potamidae) is fragmented into two chromosomes

Wang-Xinjun Cheng[1], Jun Wang[1], Mei-Lin Mao[1], Yuan-Biao Lu[1] and Jie-Xin Zou[1,2*]

Abstract

Background China is the hotspot of global freshwater crab diversity, but their wild populations are facing severe pressures associated with anthropogenic factors, necessitating the need to map their taxonomic and genetic diversity and design conservation policies.

Results Herein, we sequenced the mitochondrial genome of a Chinese freshwater crab species *Bottapotamon fukienense*, and found that it is fragmented into two chromosomes. We confirmed that fragmentation was not limited to a single specimen or population. Chromosome 1 comprised 15,111 base pairs (bp) and there were 26 genes and one pseudogene (pseudo-*nad1*) encoded on it. Chromosome 2 comprised 8,173 bp and there were 12 genes and two pseudogenes (pseudo-*trnL2* and pseudo-*rrnL*) encoded on it. Combined, they comprise the largest mitogenome (23,284 bp) among the Potamidae. *Bottapotamon* was the only genus in the Potamidae dataset exhibiting rearrangements of protein-coding genes. *Bottapotamon fukienense* exhibited average rates of sequence evolution in the dataset and did not differ in selection pressures from the remaining Potamidae.

Conclusions This is the first experimentally confirmed fragmentation of a mitogenome in crustaceans. While the mitogenome of *B. fukienense* exhibited multiple signs of elevated mitogenomic architecture evolution rates, including the exceptionally large size, duplicated genes, pseudogenisation, rearrangements of protein-coding genes, and fragmentation, there is no evidence that this is matched by elevated sequence evolutionary rates or changes in selection pressures.

Keywords Mitogenome, Fragmentation, Gene duplication, Protein-coding gene rearrangements, Crustacean, Freshwater crabs, Selection pressure, Architecture, Evolutionary rate

*Correspondence:
Jie-Xin Zou
jxzou@ncu.edu.cn
[1]Research Laboratory of Freshwater Crustacean Decapoda & Paragonimus, School of Basic Medical Sciences, Nanchang University, Nanchang, Jiangxi Province 330031, China
[2]Provincial Key Laboratory for Drug Targeting and Drug Screening, Jiangxi Medical College, Nanchang University, Nanchang 330031, China

Background

Mitochondria of bilaterian animals are commonly a single, closed, circular compact molecule, ranging from about 14 to 16 kb in size, highly conserved in terms of gene content and organization [1]. However, isolated lineages exhibit rapidly evolving and unorthodox mitochondrial architectures; in very rare cases, even mitogenomes fragmented into multiple chromosomes. Mitogenome fragmentation has occurred independently in several bilaterian lineages. For example, most rotifer species for which data are available possess mitogenomes fragmented into two chromosomes [2, 3]. Fragmentation was also reported in parasitoid wasps in the genus *Conostigmus* (Insecta: Hymenoptera) [4], and nematodes in the genus *Globodera* (Nematoda: Tylenchida) [5, 6]. Most famously, mitogenome fragmentation is widespread in lice (Insecta: Psocodea), many of which possess mitogenomes fragmented into a varying number of minichromosomes (sometimes as many as 20) [7–10]. The relationship between fragmentation and gene order rearrangement rate is unclear; there is some evidence that lice with fragmented mitogenomes also exhibit highly elevated gene order rearrangement rates, but no evidence was found that a high rearrangement rate necessarily causes mitogenomic fragmentation [11]. In addition, as gene order rearrangements and size expansions should be selectively constrained [12, 13], mitogenomic size, rearrangement rate, and sequence evolution should all be positively correlated [14].

Crustaceans exhibit strong evolutionary heterogeneity in the rate of architectural rearrangements, with some lineages exhibiting mitogenomic architecture almost perfectly conserved over hundreds of millions of years, and others exhibiting rapidly evolving mitogenomes where no two species exhibit the same gene arrangement, such as Isopoda [15–17]. While the vast majority of crustaceans exhibit the standard organization of the mitogenome into a single circular molecule [17], some isopod species exhibit highly destabilized mitogenomic organization, including phenomena such as linearization and dimerization [18, 19], and heteroplasmy (multiple mitotypes existing within a single individual) and fragmented mitogenomic phenotypes have been proposed in *Callinectes sapidus* (Decapoda) [20]. However, fragmented mitogenomes have not been experimentally confirmed in crustaceans yet.

Potamidae (Brachyura) are a large freshwater crab family comprising more than 500 described species classified into 78 genera [21, 22]. China is the global hotspot of freshwater crab diversity, with multiple new species described in the last two decades [22–25]. As a result of the destruction of ecological habitats and climate changes brought on by the Anthropocene, freshwater crab populations in China are facing severe challenges [22]. As a part of the major research project aimed at assessing the diversity of freshwater crabs and designing conservation measures necessary for their long-term survival [26], our research team has also sampled one specimen of *Bottapotamon fukienense* Dai & Lin, 1979, one of the eight recognized species in this genus of freshwater crabs predominantly distributed in China [24]. To contribute molecular data necessary for the understanding of the phylogeny and evolution of freshwater crabs, we sequenced and analysed its mitochondrial genome.

Methods

In this study, we sequenced, assembled, annotated and comparatively analysed the complete mitochondrial genome of *B. fukienense*.

Specimen collection

Ten freshwater crab specimens were collected from Xibiao Village, Dongping Town, Nanping City, Fujian Province, China in November 2008 (GPS: 118.5716/27.4548). Specimens were preserved in 95% ethanol and stored at 4 °C at the Department of Parasitology of the Medical College of Nanchang University (NCU MCP), Jiangxi, China. The authors compared collected specimens with holotype photos from the Institute of Zoology, Chinese Academy of Sciences, in Beijing, China. On the basis of this analysis, four specimens (2 adult males and 2 adult females) were identified as *B. fukienense* (Fig. 1, Additional file 1: Figure S1). To confirm that this mitogenome is fragmented across the entire species, we conducted another sampling trip in November 2021. Three specimens (2 adult males and 1 adult female) were collected from Qintang village, Aojiang Town, Lianjiang County, Fujian Province, China (GPS: 119.5085/26.2247). The identity of specimens was again morphologically confirmed against the original holotype specimen of *B. fukienense.* All experiments were conducted on unprotected invertebrates, so no permits were required for the study.

Mitogenome sequencing and assembly

Mitogenome sequencing and assembly were conducted roughly following the procedure described before [15]. The sample was rinsed in distilled water, and DNA was isolated from muscle tissue using AidLab DNA extraction kit (AidLab Biotechnologies, Beijing, China). Primers (Table 1) were designed according to the conserved regions of mitochondrial genes from available orthologues. To avoid sequencing artefacts and ensure that mitogenomes are complete and circular, primers were designed to overlap by approximately 100 bp and used to amplify and sequence the entire mitogenome. PCR reaction mixture (50 μl): 5 U μl−1 TaKaRa LA Taq polymerase (TaKaRa, Japan), 10 × LATaq Buffer II, 2.5 μM dNTP mixture, 0.2–1.0 μM each primer and 60 ng DNA

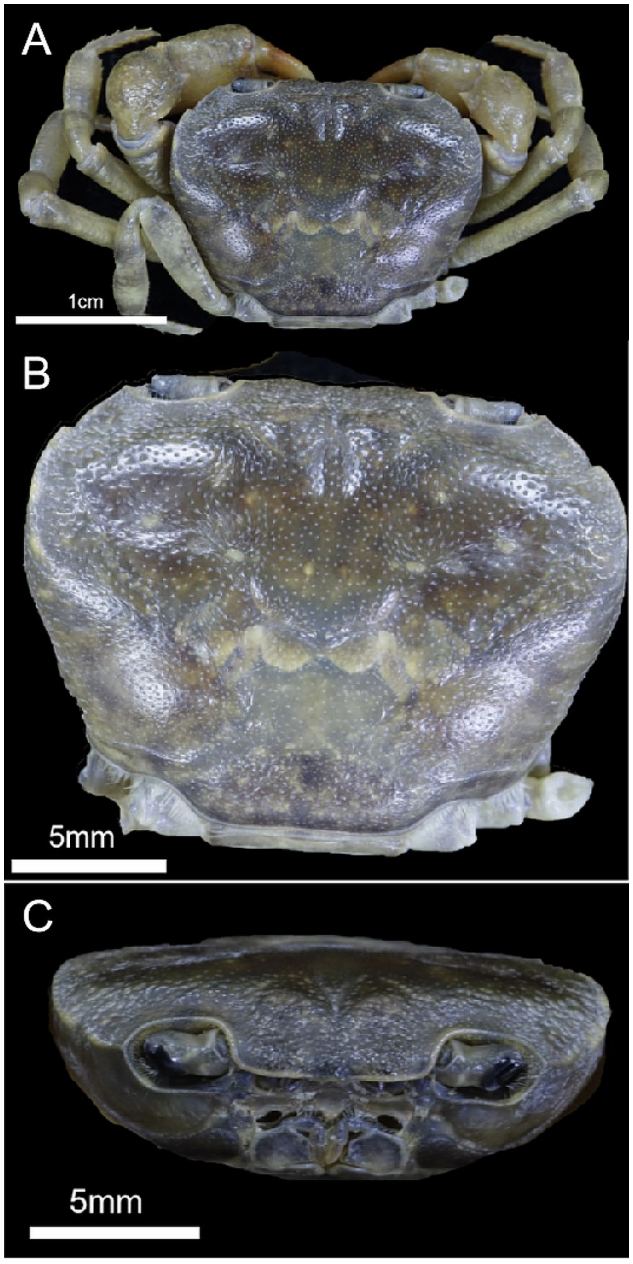

Fig. 1 Photographs of a sampled *Bottapotamon fukienense* specimen. (**A**) Dorsal view of the entire specimen. (**B**) Dorsal view of the cephalothorax. (**C**) Frontal view of the cephalothorax. Size bars are shown in each panel

template. The PCR conditions were as follows: denaturation 98 °C/2 min, 40 cycles of 98 °C/10 s, 50 °C/15 s and 68 °C/1 min kb^{-1}. When the product was not specific enough, PCR conditions were optimized by increasing the annealing temperature and decreasing the number of cycles. PCR products were sequenced using the Sanger method and the same set of primers. After quality proofing via the visual inspection of electropherograms and identity confirmation using BLAST [27], the sequences were assembled using DNASTAR v. 7.1 [28], ensuring that overlapping segments of amplicons are identical.

As results indicated a fragmented mitogenome, to confirm this unusual architecture, we collected a new specimen in 2021, and used the DNA to conduct long-range PCR using a new set of primers (other parameters were the same as above), designed to produce fragments 7 to 8 Kbp in size (Table 1).

Mitogenome annotation

Mitogenome was annotated using inputs of multiple programs: MITOS [29], DNASTAR, and ARWEN (for tRNAs) [30]. Annotations were then manually fine-tuned according to the orthologous sequences using BLAST and BLASTx. PhyloSuite [31] was used to parse and extract the annotation and to generate the file for submission to NCBI's GenBank.

Comparative and phylogenetic analyses

All 148 available (January 2024) Potamidae mitogenomes were downloaded from GenBank and imported into PhyloSuite. After the removal of all duplicated and unannotated mitogenomes, as well as leaving one mitogenome per species, 42 mitogenomes were left in the dataset. PhyloSuite was used to semi-automatically re-annotate ambiguously annotated tRNA genes with the help of the ARWEN output, uniformise annotation, extract mitogenomic features, translate genes into amino acid sequences, calculate base composition and skews, generate comparative tables, concatenate the alignments, and prepare input files for plug-in programs used for phylogenetic analyses. Two datasets were tested for phylogenetic analyses: concatenated nucleotide and amino acid sequences of 13 mitochondrial protein-coding genes (PCGs). In the former dataset, 17 sequences failed the compositional homogeneity test in IQ-TREE [32], but in the latter dataset, no sequences failed it. As compositional heterogeneity can strongly interfere with phylogenetic reconstruction [33, 34], amino acids were selected to reconstruct phylogenies. Genes were aligned in batch mode using the accurate g-INS-i strategy in MAFFT [35]. The best data partitioning scheme and best-fit evolutionary models for each partition were selected using the Bayesian Information Criterion implemented in ModelFinder [36]: mtVer+F+R4 for the *atp6-cox2-cytb-nad3* partition, LG+F+I+G4 for *atp8*, Q.plant+F+R3 for *cox1-cox3*, mtVer+F+I+I+R3for *nad1-nad4L*, mtVer+F+R4 for *nad2-nad6*, and mtVer+F+R4 for *nad4-nad5*. Phylogenies were inferred using two algorithms: the Maximum Likelihood (ML) methodology implemented in IQ-TREE, and the Bayesian inference (BI) implemented in MrBayes [37]. We assessed the support for the ML topology using 20,000 UltraFast Bootstrap [38] replicates. The Bayesian inference analysis was conducted as two independent runs (four chains each), and the average standard deviation of split frequencies

Table 1 Primers used for amplification and sequencing of the mitochondrial genome of *B. Fukienense*. "Fragment" indicates the fragment number, and "Genes" the mitochondrial genes that amplified sequence spanned

Fragment	Genes	Name	Sequence (5'-3')	Length (bp)
Standard PCR				
F1	16 S	XX16SF	GGTTTGAACTCAAATCATG	479
		XX16SR	TRACYGTGCRAAGGTAGCAT	
F2	16 S-COX2	BT1F1	CAATGTAAAGTTTTATAGGGTC	2798
		BT1R1	ACATCTGCTGCAGTAATGAG	
F3	COX2	XXCOX2F	GGHCAYCARTGATATTGAAG	296
		XXCOX2R	CCRCARATYTCWGARCAYTGNCC	
F4	COX2-ATP6	BT1F2	CACTCATGAACCATTCCC	771
		BT1R2	CATAAGGTAGGAGTCCTAGG	
F5	ATP6	XXATP6F	CGATGATCTCTCCTCTGAAG	284
		XXATP6R	GGAGGAGTACCTTGGGGTAC	
F6	ATP6-NAD5	BT1F3	CTTTGTCTCTTCCTCTTTG	4000
		BT1R3	TTAGGTTGGGATGGGTTAGG	
F7	NAD5-NAD4	BT1F4	CTATTAACCCAATTCTTG	1363
		BT1R4	GTGGGTTAGGAATAAATGAAAGG	
F8	NAD4	XXND4F	GGVGCYTCNACATGNGCYTTWGG	260
		XXND4R	GGWTGRGGNTAYCARCCHGARCG	
F9	NAD4-CYTB	BT1F5	CCTTTCATTTATTCCTAACCCAC	1898
		BT1R5	CTGTGGCACCTCAGAAGG	
F10	CYTB	XXCYTBF	CAAGAGTCACCCATATTTGCC	866
		XXCYTBR	TTGGCCAGTAAGAACGTAAGG	
F11	CYTB-16 S	BT1F6	ACCTTTTACTCATTCCTC	3726
		BT1R6	GAGTTCTTATCGAAAAAGAAG	
Chromosome 2				
F1	16 S	XX16SF	GGTTTGAACTCAAATCATG	479
		XX16SR	TRACYGTGCRAAGGTAGCAT	
F2	16 S-COX1	BT1F1	CAATGTAAAGTTTTATAGGGTC	4877
		BT2R7	GCTATATCTGGAGCTCCTAA	
F3	COX1	XXCOX1F	GCWTGAKCWGGHATAGTDGGNAC	1255
		XXCOX1R	CDGARTAWCGWCGHGGYATHCC	
F4	COX1-16 S	BT2F8	GGAATTACCCACTGATTTTC	2207
		BT1R6	GAGTTCTTATCGAAAAAGAAG	
Long-range PCR				
Chromosome 1				
F1	CYTB-ATP6	BT1F6	ACCTTTTACTCATTCCTC	7697
		BT3R9	GAACAGCTAAGGTCCCAGGACG	
F2	ATP6-CYTB	BT1F3	CTTTGTCTCTTCCTCTTTG	7708
		BT3R10	GAACGTAAGGCGATTCTAC	
Chromosome 2				
F1	COX1	BT3F8	GGAATTACCCACTGATTTTC	7278
		BT2R7	GCTATATCTGGAGCTCCTAA	

(SDSF) was used to determine the needed number of generations. SDSF values < 0.01, which indicates convergence, were reached after ≈55,000 generations. The SDSF values more or less plateaued after that, so the analysis was allowed to continue till 150,000 generations (SDSF = 0.0085). The first 25% of sampled trees were discarded as burn-in. Phylogenetic studies mostly indicate Gecarcinucidae as the sister family to Potamidae [17, 39, 40], so the only two available mitogenomes (both *Esanthelpusa*) for this family were used as the outgroup (Potamonautidae, the third Old World freshwater crab clade was not available). TreeSuite function in PhyloSuite 1.2.3 [41] was used to extract branch lengths, and infer the relative composition variability values (RCV), spurious species, and long-branch scores [42]. UGENE was used to infer pairwise differences among genes and generate figures of alignments [43]. For tRNA folding and visualization, we used RNAfold and *forna* tools of

the ViennaRNA Web Services [44]. Tandem repeats were inferred using Tandem Repeats Finder [45]. OGDRAW was used to draw circular mitogenomic maps [46]. RELAX HyPhy tool was used to infer selection pressures; this tool introduces the K parameter, where K>1 values indicate intensified selection and K<1 values indicate relaxed selection [47].

Results

Mitogenomic architecture

By relying on the criterion of identical overlapping segments of amplicons, we found that the sequenced mitogenomic fragments of *B. fukienense* could not be assembled into a single circular mitogenome. Instead, they assembled into two circular chromosomes (Fig. 2; Table 2). More specifically, although the first circular chromosome was assembled completely, it was smaller than expected, was missing genes, and some of the PCR segments could not be incorporated into it. However, the remaining sequenced fragments could be assembled into another circular chromosome. To confirm that the fragmentation is not accidental, and limited to only one specimen or lineage, we sampled a new set of specimens from a different locality (>100 km distant from the first locality). The DNA extracted from the new specimen was used to conduct long-range PCR using primers designed anew according to the mitogenomic sequence of *B. fukienense* obtained in previous steps (Table 1). The results produced using this approach confirmed that the mitogenome of this species is fragmented into two circular chromosomes (Fig. 3). Chromosome 1 comprised 15,111 base pairs (bp) and there were 26 genes and one pseudogene (pseudo-*nad1*) encoded on it (Additional file 1: Figure S2). Chromosome 2 comprised 8,173 bp and there were 12 genes and two pseudogenes (pseudo-*trnL2* and pseudo-*rrnL*) encoded on it (Additional file 1: Figure S3).

Several genes were duplicated when the entire mitogenome was considered (Fig. 2; Table 2). We found two copies of *nad1*, one on each chromosome: the copy on chromosome 2 (the smaller one) was the functional one, as the copy on chromosome 1 was truncated by approximately 230 bases. Remarkably, the first 703 bases were almost perfectly conserved between the two copies, which indicates a recent duplication. The complete gene was highly conserved compared to other Potamidae orthologues.

A copy of *rrnL* (or *16S*) was present on both chromosomes: a complete gene on chromosome 1 (1326 bp), and a truncated pseudogene on chromosome 2 (752 bp). The copy on chromosome 1 was highly conserved in comparison to most other Potamidae orthologues, whereas the copy on chromosome 2 comprised only the second half of the gene (5'-end-truncated). However, the matching segments of the two copies were also almost perfectly conserved (1 SNP). We checked whether the intergenic space adjacent to pseudo-*rrnL* corresponds to *rrnL*, but the two sequences could not be aligned, confirming that this is a deletion and not sequence degradation.

There were also two copies of *rrnS* (or *12 S*): *rrnS-1* on chromosome 1 (822 bp) and *rrnS-2* on chromosome 2 (823 bp). There were about a dozen SNPs between the two copies (1% divergence). In comparison to the congeneric *Bottapotamon lingchuanense*, both sequences exhibited 10% divergence. In comparison to other orthologues, the *rrnS-1* exhibited a marginally more conserved sequence.

There were two copies of *trnL1*: one on each chromosome. They exhibited 100% identity, and they were highly conserved in comparison to most other orthologues.

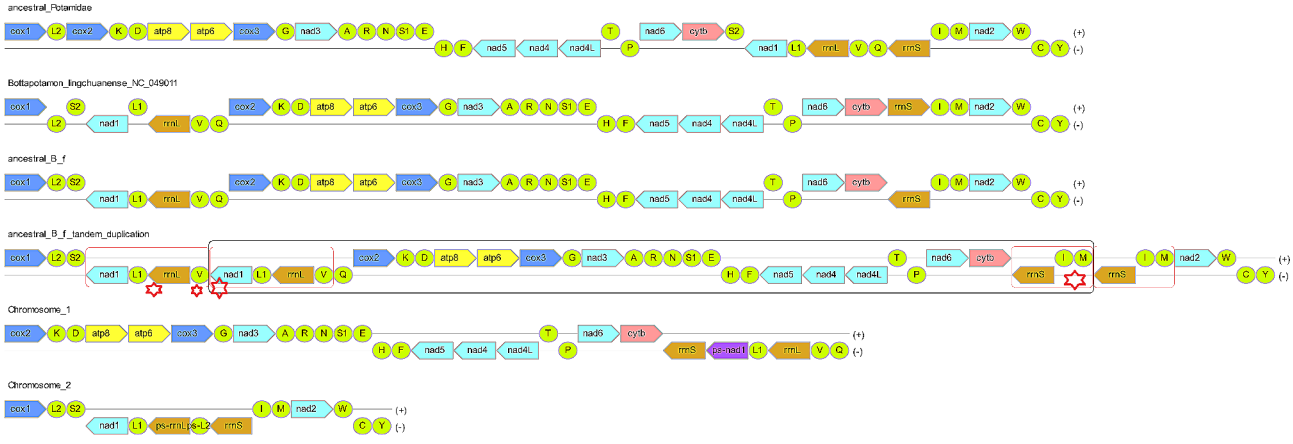

Fig. 2 The mitogenomic architecture of *B. fukienense* and the hypothetical scenario of mitogenome fragmentation into chromosomes 1 and 2. The "ancestral_Potamidae" sequence was inferred by [25], and the "ancestral Bottapotamon_fukienense" architecture was inferred by us. Putative tandem duplication events in the ancestral *B. fukienense* architecture are indicated by red squares, and chromosome 1 is indicated by a black square. Sequence deletions and gene pseudogenisation events are indicated by star symbols. The figure was made using PhyloSuite.

Table 2 Detailed architecture of the two mitogenomic chromosomes of *Bottapotamon fukienense*. IGR is the intergenic region, where negative values indicate overlaps

Gene	Position		Size	IGR	Codon		Anti-codon	Strand
	From	To			Start	Stop		
Chromosome 1								
rrnL	1	1326	1326					L
trnV	1327	1398	72				TAC	L
trnQ	1868	1936	69	469			TTG	L
cox2	2728	3405	678	791	ATG	TAA		H
trnK	3411	3477	67	5			CTT	H
trnD	3479	3543	65	1			GTC	H
atp8	3544	3705	162		ATG	TAG		H
atp6	3702	4373	672	-4	ATA	TAA		H
cox3	4373	5164	792	-1	ATG	TAA		H
trnG	5170	5234	65	5			TCC	H
nad3	5235	5586	352		ATT	T		H
trnA	5587	5653	67				TGC	H
trnR	5655	5716	62	1			TCG	H
trnN	5716	5780	65	-1			GTT	H
trnS1	5786	5852	67	5			TCT	H
trnE	5866	5931	66	13			TTC	H
trnH	6506	6568	63	574			GTG	L
trnF	6569	6630	62				GAA	L
nad5	6633	8361	1729	2	ATG	T		L
nad4	8408	9745	1338	46	ATG	TAA		L
nad4L	9739	10,041	303	-7	ATG	TAA		L
trnT	10,044	10,107	64	2			TGT	H
trnP	10,108	10,171	64				TGG	L
nad6	10,174	10,677	504	2	ATT	TAA		H
cytb	10,677	11,813	1137	-1	ATG	TAA		H
rrnS-1	12,748	13,569	822	934				L
pseudo-*nad1*	14,308	15,012	705	738	ATA	TAA		L
trnL1-1	15,041	15,107	67	28			TAG	L
Chromosome 2								
pseudo-*rrnL*	5	752	748	4				L
pseudo-*trnL2*	1275	1336	62	522			TAA	L
rrnS-2	1337	2159	823					L
trnI	3592	3663	72	1432			GAT	H
trnM	3747	3812	66	83			CAT	H
nad2	3813	4817	1005		ATG	TAA		H
trnW	4816	4880	65	-2			TCA	H
trnC	4880	4941	62	-1			GCA	L
trnY	4942	5004	63				GTA	L
cox1	5009	6547	1539	4	ATG	TAA		H
trnL2	6543	6604	62	-5			TAA	H
trnS2	6877	6945	69	272			TGA	H
nad1	7140	8078	939	194	ATA	TAA		L
trnL1-2	8107	8173	67	28			TAG	L

Initial analyses indicated the presence of putative two *trnL2* copies on chromosome 2 (Table 2). One copy (annotated as *trnL2*) was found in the ancestral position, between *cox1* and *trnS2*, whereas the other copy (annotated as pseudo-*trnL2*) was found between *rrnL-2* and *rrnS*-2. The alignment with orthologues revealed that *trnL2* (found in the ancestral position) exhibited high levels of homology, whereas pseudo-*trnL2* exhibited almost no homology (Additional file 1: Figure S4). This indicated a possibility of an annotation artefact. Considering the

Fig. 3 Electrophoresis confirmation of fragmentation into two chromosomes in the mitochondrial genome of *B. fukienense*. From left to right: 1 kb DNA ladder, with sizes in bases shown; chr1-F1: Chromosome 1, fragment 1 (*cytb* to *atp6*, 7697 bases); chr1-F2: Chromosome 1, fragment 2 (*atp6* to *cytb*, 7708 bases); chr2-F1: Chromosome 2, fragment 1 (*cox1* to *cox1*, 7278 bases); *cox1* (1255 bases, primers XXCOX1F and R). For primers, see Table 1

ancestral architecture of this gene (Fig. 2), we assumed that the gene might be a degraded *trnV*. Indeed, the alignment of pseudo-*trnL2* with *trnV* genes of Potamidae revealed a high level of homology, but also a large deletion, probably rendering it non-functional (Additional file 1: Figure S5). However, the ARWEN algorithm annotated it as *trnL2* and successfully folded both sequences into cloverleaf structures (Additional file 1: Figure S6). We further applied the RNAfold and *forna* tools of the ViennaRNA Web Services, but they failed to produce a standard cloverleaf structure for either of the two genes (Additional file 1: Figure S7). In light of the above analyses, we cannot be certain whether this was a case of tRNA remodelling and the gene is functional, or whether

the deletion in the ancestral *trnV* gene caused a loss of functionality and produced accidental similarity to *trnL2*.

In order to attempt to infer the putative evolutionary history of architectural rearrangements that led to the observed mitogenomic architecture of *B. fukienense*, we compared it to the ancestral gene order for Potamidae [25] (Fig. 2), exhibited by most species in our comparative dataset (e.g. *Huananpotamon lichuanense*) (Fig. 4). We also included the gene order of the closest-related available species, *B. lingchuanense*, as it differed from the ancestral gene order. Notably, this is most likely to be the ancestral order of the clade comprising both the *Bottapotamon* and *Neilupotamon* genera, as it was found in most of the *Neilupotamon* species (Fig. 4). The comparison of the two chromosomes with these two gene orders showed that *B. fukienense* exhibits a gene order highly similar to *B. lingchuanense* (Fig. 2). A large section of chromosome 1 perfectly corresponded to the large section of *B. lingchuanense* mitogenome, spanning pseudo-*nad1-L1-rrnL-V-Q-cox2-K-D-atp8-atp6-cox3-G-nad3-A-R-N-S1-E-H-F-nad5-nad4-na4L-T-P-nad6-cytb-rrnS* genes. A fragment comprising *rrnS-I-M-nad2-W-C-Y-cox1-L2-S2-nad1-L1-rrnL-pseudo-L2* formed chromosome 2. We inferred the ancestral gene order of *B. fukienense* as being almost identical to the gene order of *B. lingchuanense*, with only differences in the strand distribution of *trnL1*, *trnL2*, and *rrnS* (Fig. 2). As their strand distribution in *B. fukienense* corresponds to the ancestral arrangement for Potamidae (Fig. 2), we propose that these three genes underwent strand switches in *B. lingchuanense*. The additional steps needed to explain the architecture of the two chromosomes comprise tandem duplications of the *nad1-L1-rrnL-V* and *rrnS-I-M* sections in the ancestral (non-fragmented) mitogenome (Fig. 2). Following this, double-stranded DNA breaks (//) occurred in two places, between both duplicated sections: *nad1-L1-rrnL-V//nad1-L1-rrnL-V* and *rrnS-I-M//rrnS-I-M*. This was followed by the circularisation of the two fragments, and a deletion of the sequence fragment comprising *trnI* and *trnM* on chromosome 1 (Fig. 2). To confirm the deletion, we compared the large non-coding region (NCR) between *rrnS* and *trnI* on chromosome 2 spanning 1432 bases, and the NCR between *rrnS-1* and pseudo-*nad1* on chromosome 1 spanning 738 bases. The alignment indicated that the sequence of the smaller NCR was highly conserved in comparison to the larger NCR (≈a dozen SNPs and deletions). This supports our hypothesis that the downstream fragment of the duplicated *rrnS-I-M* segment was lost during the fragmentation and recircularization, causing the loss of *trnI* and *trnM* genes from chromosome 1. The only extra step required to produce the two chromosomes was the conversion of the ancestral *trnV* on chromosome 2 into pseudo-*trnL2*, as discussed above.

We further tested the hypothesis that the existence of tandem repeats may facilitate intramolecular recombination of strand slippage of replication machinery [48]. Tandem repeats were identified in two large NCRs on chromosome 1: 791 bp between *trnQ* and *cox2*, and 574 bp between *trnE* and *trnH*. In the 791 bp NCR, there were two tandem repeats: 18×2 bases and 12×9 bases.

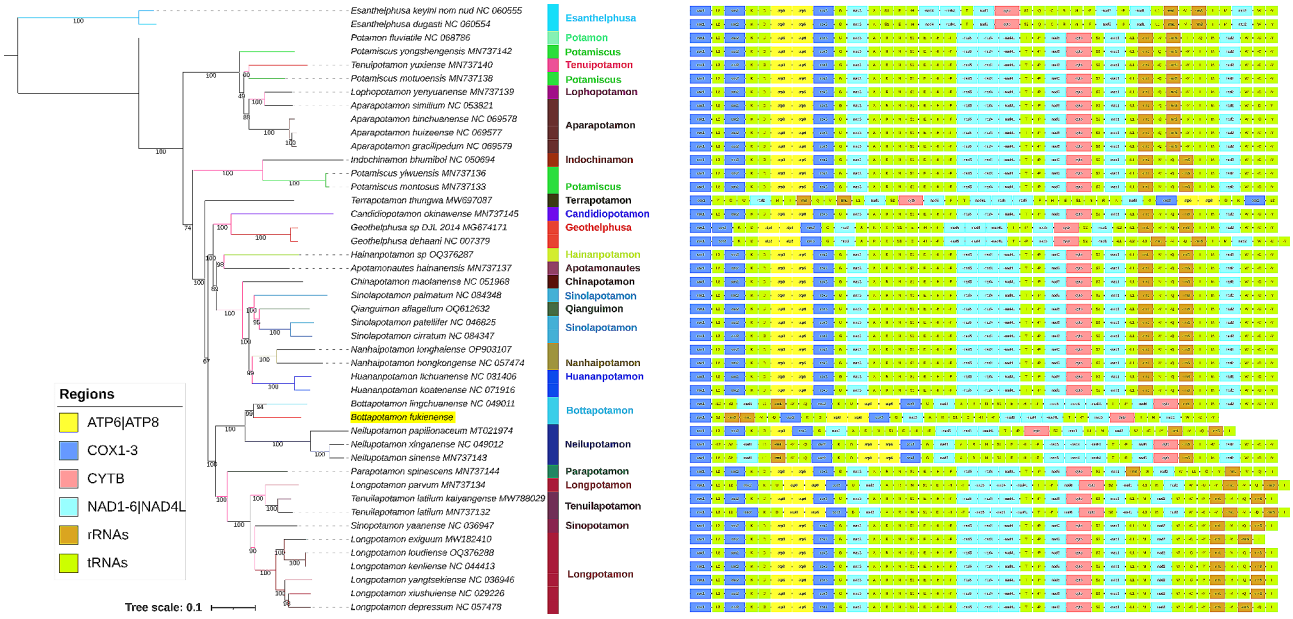

Fig. 4 The mitogenomic architecture and Maximum Likelihood phylogeny of Potamidae inferred using amino acid sequences of 13 mitogenomic protein-coding genes. Bootstrap support values < 100 are shown at nodes. *Esanthelpusa* is the outgroup. Two chromosomes of *B. fukienense* are merged into a single mitogenome

In the 574 bp NCR, there were seven different tandem repeats: 76×2 bases, 19×8 bases, 3.4×47 bases, 19×12 bases, 7.5×36 bases, 30×12 bases, and 17.4×10 bases (Additional file 1: Table S1). These two NCRs do not correspond to regions where putative sequence duplication and mitogenome fragmentation events took place, although the 791 bp NCR is in the proximity of a putative tandem duplication region, comprising *nad1-L1-rrnL-V*, upstream from *trnQ*.

Gene order rearrangements and sequence evolution

We merged the two chromosomes of *B. fukienense* into a single mitogenome and conducted a range of comparative mitogenomic architecture analyses to assess whether it exhibits any other unique evolutionary features, aside from fragmentation and duplication of multiple genes. While gene orders were generally conserved in Potamidae, the two available *Bottapotamon* species exhibited highly rearranged gene orders (Fig. 4). More precisely, the clade comprising two *Bottapotamon* and three *Neilupotamon* species was the only one exhibiting rearrangements of protein-coding genes in comparison to the ancestral arrangement, observed in most Potamidae mitogenomes (Figs. 2 and 4). The sister clade to these two genera, comprising *Parapotamon*, *Sinopotamon*, *Tenuilapotamon*, and *Longpotamon* genera, exhibited the ancestral PCG order, but the common ancestor of the clade underwent a translocation of two rRNA genes together with a block of tRNA genes. Among the species from the remaining 16 genera, only minor rearrangements in tRNA genes in comparison to the ancestral architecture were observed. Therefore, there are indications of progressively elevated mitochondrial architecture rearrangement rates within the clade comprising these six genera, culminating with the fragmented mitogenome in *B. fukienense*. The evolutionary scenario of rearrangements is unclear, as all species apart from *Neilupotamon papilionaceum* exhibit the same PCGs+rRNAs order (notwithstanding gene duplications and fragmentation in *B. fukienense*), with the large box comprising *S2-nad1-L1-rrnL-V-Q* genes translocated between *cox1-L2* and *cox2* genes. However, *N. papilionaceum* exhibits the ancestral arrangement of the above gene box, but with the *M-nad2-W-C-Y* gene box translocated within it, between *nad1-L1* and *rrnL*. As we can infer with confidence the existence of annotation and assembly errors in the mitogenome of *N. papilionaceum* (*atp6* and *nad6* were not annotated, and at 16,273 bases, the mitogenome was much smaller than mitogenomes of related species, which indicates that it might be incomplete), we also cannot exclude assembly errors. It is necessary to sequence more species belonging to these two genera with fast-evolving mitogenomic evolution.

To test the hypothesis that elevated architectural rearrangement rate and ultimately fragmentation are associated with relaxed purifying selection pressures (i.e. higher overall evolutionary rates), we compared evolutionary rates (branch lengths) among different lineages. *Bottapotamon fukienense* exhibited an average branch length among the Potamidae (0.393; average=0.389). As a result of the relatively narrow range of branch lengths in the dataset (0.330 and 0.414), no spurious species were identified in the dataset. We further confirmed this using long-branch scores, which ranged from −18.8 to 34.6 in Potamidae, and *Bottapotamon fukienense* (-6.3) exhibited a lower-than-average value within the dataset (average≈0). Similarly, the relative composition variability values (RCV) were low across the dataset (0.017 to 0.049), aside from the major outlier of *N. papilionaceum* (0.215). As this species exhibited two missing genes, this is the most likely underlying reason for this orders-of-magnitude increase in RCV. *Bottapotamon fukienense* exhibited an average RCV (0.026) within the Potamidae dataset (average=0.028; the outlier excluded). Finally, we compared branch lengths between the "fast-evolving" clade comprising the six genera exhibiting relatively rapidly evolving architecture and the remaining 16 "conserved" genera. Again, branch lengths were almost identical between the two clades (0.397 vs. 0.393 respectively; df=41, t-value=0.66, p-value=0.51).

To further test the hypothesis that fragmentation is associated with relaxed purifying selection pressures, we also conducted selection tests. With *B. fukienense* selected as the test branch, and all other Potamidae as background, the test of differences in selection pressures between the two groups was nonsignificant (K=0.94, p=0.68, LR=0.18). With the two *Bottapotamon* species selected as the test branches, and all other Potamidae as background, the test of differences in selection pressures between the two groups was nonsignificant (K=1.02, p=0.75, LR=0.10). With the group of six genera with elevated architectural evolutionary rates selected as test branches, the RELAX algorithm found significant (p=0.001, LR=12.09) evidence of selection intensification in test branches.

To test the hypothesis that elevated architectural rearrangement rates are associated with increased mitogenome size, we compared mitogenome size among the Potamidae. These analyses can be strongly affected by sequencing and assembly artefacts, so our findings must be interpreted with these limitations in mind. As *N. papilionaceum* was missing multiple genes and exhibited a small size, we removed it from the dataset. Potamidae exhibited large mitogenomes on average (17.5 Kbp), but when we merged the two *P. fukienense* chromosomes into a single mitogenome, it exhibited the largest size (23,284 bp) among the Potamidae (Additional file 2: Sheet S1). It was much larger than the second-largest described Potamidae mitogenome: *Parapotamon*

spinescens with 20,027 bp (notably, this mitogenome was incomplete) [25]. Aside from gene duplications, this exceptional size was also a product of this species exhibiting by far the highest ratio of NCRs within the dataset: 34.6%, followed by *Parapotamon spinescens* at 26.4% (Additional file 2: Sheet S1). Combined, the four species from the two genera with fast-evolving architecture, *Bottapotamon* and *Neilupotamon*, exhibited significantly larger mitogenomes than the remaining lineages (19,186 vs. 17564, df=40, t-value=2.081, p-value=0.044). The six genera exhibiting relatively fast architecture evolution also exhibited significantly larger mitogenomes than the remaining lineages (18,670 vs. 17,133, df=40, t-value=3.555, p-value=0.001).

In terms of base composition, the mitogenome (both chromosomes merged) of *B. fukienense* exhibited a high, but average within the dataset, AT bias of 73.1% (Additional file 2: Sheet S1). The G-base content was the second smallest within the dataset (8.0%) after only *Parapotamon spinescens* (7.7%). It had a low AT skew (-0.007), but the largest GC skew in the dataset (-0.408). However, GC skew magnitude was not exceptional, as the range in the remainder of the dataset was from −0.222 to -0. 399. *Terrapotamon thungwa* (MW697087) exhibited a fully inverted GC skew (0.32), but this was an artefact caused by the authors submitting the minority strand to the GenBank (Fig. 4). There were no other species exhibiting skew inversions in the dataset.

Start and stop codons were highly conserved and standard in PCGs of *B. fukienense*: ATA, ATG, ATT, and TAG, TAA, T– respectively (Table 1, Additional file 2: Sheet S2). In terms of length and sequence, most PCGs were highly conserved across the entire family. *Atp8* was remarkably conserved in both aspects across the Potamidae (159 bp in all available species). This is unusual, as this is commonly the fastest-evolving mitochondrial PCG [49]. Intriguingly, *B. fukienense* was the only exception in terms of length of *atp8*, with 162 bases, caused by a single amino acid insertion (S; TCT base triplet) (Additional file 1: Figure S8). *Cox1* exhibited an elongation comprising a single base triplet at the 3'-end (TTA), but this was shared by *B. lingchuanense* and three other closely related species. *Nad2* was highly conserved in comparison to other orthologues in *B. fukienense*, but in congeneric *B. lingchuanense*, it exhibited a large 15 amino acids insertion and a smaller one of 3 amino acids near the 5'-end. Other PCGs were highly conserved.

Overlaps between genes were small (≤2 bases), apart from the *nad4-nad4L* and *atp6-atp8* pairs of genes, which commonly overlap in many animal species [1]. Surprisingly, *trnL2* overlapped with *cox1* by 5 bases, which is uncommon, as *cox1* is a highly conserved gene. However, this overlap is conserved across many Potamidae [25].

In terms of phylogenetic relationships of the remaining lineages, *Potamiscus* was paraphyletic in both ML and BI topologies, with *Potamiscus yongshengensis* and *Potamiscus motuoensis* clustering with *Tenuipotamon*, *Lophopotamon* and *Aparapotamon*, but their exact positions varied between the two topologies (Fig. 4 and Additional file 1: Figure S9). The paraphyly of this genus is a known problem [50]. *Longpotamon* was also paraphyletic, with *Longpotamon parvum* comprising a sister lineage to *Tenuilapotamon latilum.* ML and BI topologies differed in the position of the *Indochinamon* lineage. The position of the *Sinopotamon* lineage differed between BI and ML topologies, and its relationship to the *L. parvum*+*T. latilum* clade.

Discussion

Herein, we sequenced the mitochondrial genome of a Chinese freshwater crab species *B. fukienense* and found that it is fragmented into two chromosomes. At the time of this study (January 2024), there was only congeneric one mitogenome available: *B. lingchuanense* [51]. It exhibited a standard architecture, but the authors failed to annotate two tRNA genes: *tRNA-Ile* and *tRNA-Met*. A recent review of all crustacean mitogenomes failed to observe a single fragmented mitogenome [17], with a minor exception of the mitogenome of the abyssal amphipod *Hirondellea gigas*, for which the authors submitted two contigs that they failed to assemble into a single mitogenome [52]. This may indicate fragmentation, but it is also possible that they simply failed to sequence noncoding regions completely, preventing the assembly of the two contigs into a circular mitogenome. In addition, heteroplasmy and a minor proportion of fragmented mitogenomic phenotypes have been proposed in *Callinectes sapidus* (Decapoda) [20], but the authors merely relied on unmapped reads to infer fragmentation and did not confirm this using additional experiments. Similarly, in a recent study of freshwater crab mitogenomes, authors found that mitogenomes of *Parapotamon spinescens* and *Tenuilapotamon latilum* could not be circularized due to sequence gaps (two in the former, one in the latter) [25]. Again, we cannot conclude whether this may be indicative of a circularisation or sequencing artefacts. Therefore, to our knowledge, this is the first experimentally confirmed fragmentation of a mitogenome in crustaceans. In addition, as opposed to results in *Callinectes sapidus*, we did not find indications of the existence of non-fragmented mitogenomic phenotypes in the DNA of *B. fukienense*. Importantly, we conducted two rounds of sampling and sampled geographically distant populations. This way we confirmed that fragmentation was not limited to a single specimen or population. In addition, the above studies relied on NGS, and there is evidence that in some cases

NGS approaches (e.g. Illumina sequencing) can produce incomplete mitogenomic assemblies [53]. Herein, we relied on Sanger sequencing, which is slower and more expensive, but it allowed us to design primers producing overlapping segments and confirm the completeness and fragmentation of this mitogenome. Notably, we also encountered multiple problems in the amplification and sequencing of this mitogenome. Particularly difficult to sequence were *nad5*, *nad2* and *trnN* genes. This may be caused by the existence of repetitive sequences [54], but also be indicative of heteroplasmy (multiple sequences existing within a single individual), which appears to be common in lineages with fragmented mitogenomes [55]. Regardless, all sequenced fragments assembled into two mitogenomic circles. Finally, a number of factors allowed us to exclude the possibility that these two mitogenomic fragments are *numts* (nuclear genome-encoded mitogenomic fragments) with high confidence, comprising circularity, large size, the absence of stop codons in PCGs, etc. [56, 57].

We also observed large sequence duplications, producing several duplicated genes (*rrnS* and *trnL1*) and pseudogenes (*nad1*, *rrnL* and *trnL2*). While duplications and expansion of noncoding regions are relatively common in crustaceans [17] and other invertebrates, such extensive gene duplications and pseudogenisations are uncommon [58]. They have been reported in several Nematoda lineages [6, 59, 60], and isolated insect [61] and reptile (lizards and salamanders) [62, 63] lineages. Our reconstruction of the ancestral mitogenomic structure for *B. fukienense* indicated that it probably underwent tandem duplications of two mitogenomic segments, spanning multiple genes. Notably, a similar tandemly duplicated region spanning multiple genes was previously observed in a decapod crustacean, *Homarus gammarus* [53]. The putative duplication mechanisms comprise the slipped-strand mispairing mechanism [64] or hybridisation of two uneven mitogenomic minicircles [4].

This also brings us to the putative mechanism leading to the observed architecture. The existence of multiple mitotypes (e.g. complete and fragmented) within a single cell and mitogenomic recombination were proposed as key parts of the mechanism explaining the evolutionary occurrence of multipartite mitogenomes in multiple lineages [4, 6, 8, 11, 55]. The generation of long-lived minicircles was also proposed as an intermediate step in explaining the high levels of gene order rearrangements if it is followed by their integration into the full-length mitogenome via homologous recombination [4]. Indeed, it has been shown that mitochondrial architecture of some lice with fragmented mitogenomes evolves by splits and mergers of minichromosomes [65]. Mao et al. [4] proposed that these minicircles should contain the origin of replication in order to be long-lived, but identification of the control region and the origin of replication in crustaceans was proven to be nearly impossible due to high levels of divergence in noncoding regions and the absence of conserved motifs associated with the origin of replication [17]. However, we did identify a highly conserved noncoding segment shared by both mitogenomic chromosomes adjacent to *rrnS*, which might comprise the control region. In indirect support of this hypothesis, genes flanking the origins of strand replication usually form hotspots of duplications [66–69], and our reconstruction of the scenario leading to the observed mitogenomic architecture proposed a duplication of the *rrnS-I-M* gene box (Fig. 2).

We found indications of increased mitogenomic architecture rearrangement rates in the clade comprising sister genera *Bottapotamon* and *Neilupotamon*. More precisely, this was the only clade that exhibited rearrangements of PCGs compared to the ancestral arrangement. In comparison to relatively variable tRNA genes, PCGs and rRNAs commonly exhibit much less variable arrangements [58, 70–72], so within-family variability in the arrangement of PCGs would be considered unusual in most bilaterian lineages [1, 58, 73]. However, it has been observed in several crustacean families; e.g. Chthamalidae, Allocrangonyctidae, Lysianassidae, Palaemonidae, Nephropidae, and Parastacidae [17, 53, 74]. Intrageneric rearrangements of genes other than tRNAs are even rarer, and a previous study reported that they are completely absent from crustaceans [58]. In this aspect, the genus *Bottapotamon*, exhibiting two different arrangements of PCGs is unique among crustaceans. This also indirectly supports the observation that fragmentation events are more common in lineages with high architectural evolutionary rates [11]. Notably, the same group of authors stressed that due to the rarity and likely randomness of fragmentation events, there is no direct correlation between the two variables.

Two studies proposed that the fragmentation of mitogenomes is associated with relaxed purifying selection pressures on mitochondrial genes and increased sequence evolutionary rates [55, 75]. Furthermore, elevated architectural evolution rates are correlated with elevated sequence evolution rates in a range of animal lineages [11, 71, 73, 76–78]. Contrary to these previous findings, we did not find any evidence of elevated mutational rates or relaxation of purifying selection pressures in *B. fukienense*, nor in the genera exhibiting rearrangements of PCG and rRNA genes. Several previous studies also reported the existence of exceptions from this presumed correlation between the sequence and architecture evolutionary rates [14, 16, 71, 79].

As a result of sequence duplications described above, *B. fukienense* also exhibited the largest mitogenome among the Potamidae. This indirectly supports the observation

that mitogenome size is often positively correlated with gene order rearrangement rate, observed in some [80], but not all [81] nematodes and flatworms [14]. The mitogenome also exhibited the highest GC skew magnitude within the available Potamidae dataset. However, as GC skew magnitude is driven primarily by the strength of purifying selection pressure [82], NCRs are expected to exhibit elevated GC skews. Therefore, the high skew in this mitogenome is most likely a consequence of the largest ratio of noncoding regions within the dataset (35%), and the associated highly relaxed purifying selection pressures. Indeed, the GC skew value on the coding section of the mitogenome was much lower (-0.313), and only slightly above the average value (-0.284; range from −0.212 to -0.367) for the entire dataset (Additional file 2: Sheet S1). This indicates that sequence duplications in this mitogenome are not of a very recent evolutionary origin, as a certain evolutionary time is presumably required for GC skew magnitude to increase even in the absence of purifying selection pressures [17, 82, 83]. Contrary to this, relatively low levels of sequence divergence between the duplicated fragments indicate that the duplication did not occur deep in the evolutionary history, so we hypothesise that it might be confined to this species. The presence of pseudogenes further supports this, as they are expected to be removed from the genome by the selection for small size relatively quickly [67]. Further samples from closely related species and additional populations of *B. fukienense* are needed to place this fragmentation more precisely in evolutionary time.

Conclusions

Fragmentation aside, the mitogenome of *B. fukienense* exhibited multiple other signs of elevated mitogenomic architecture evolution rates, including the exceptionally large size, duplicated genes, pseudogenisation, and high PCG rearrangement rate, but there is no evidence that this is matched by elevated sequence evolutionary rates or changes in selection pressures. As genomic rearrangements are random evolutionary events, we can speculate with relative confidence that the fragmentation event itself was a nonadaptive evolutionary accident. However, this species clusters within a clade of Potamidae exhibiting progressively elevated architecture rearrangement rates and mitogenomic sizes, culminating with fragmentation in *B. fukienense*. This overall trend is indicative of elevated architectural dynamics, likely associated with mutations in mitogenomic replication and maintenance machinery encoded in the nuclear genome [71, 84]. The evolutionary future of this fragmentation is unclear. On one hand, small mitochondrial genomes (chromosomes) are believed to have transmission advantages over large genomes/chromosomes due to shorter replication time [7, 55, 85], the fact that the vast majority of animals do not possess fragmented mitogenomes indicates that purifying selection acts against mitogenomic fragmentation. Indeed, given the central role of locomotory capacity in the strength of purifying selection acting on mitochondrial genomes [82, 86, 87], it appears to make sense that a lineage with low locomotory capacity, lice, is the only one with evolutionarily widespread fragmentation of mitochondrial genomes. This may indicate that a *B. fukienense* phenotype with a complete mitogenome (arising randomly through hybridisation) might have an evolutionary advantage over the fragmented phenotype, and that this species may revert to the ancestral state in its evolutionary future. Continued genetic monitoring of populations of this species might offer novel and important insights into the mitochondrial evolutionary dynamics.

Abbreviations

BI	Bayesian Inference
bp	Base pair
Kbp	Kilo base pair
ML	Maximum Likelihood
NCR	Non-coding region
PCG	Protein-coding gene
RCV	Relative composition variability
SDSF	Standard deviation of split frequencies
SNP	Single-nucleotide polymorphism

Supplementary Information

The online version contains supplementary material available at https://doi.org/10.1186/s12864-024-10657-9.

Supplementary Material 1

Supplementary Material 2

Acknowledgements

We are grateful to You-Zhu Cheng, Wei-Ping Wu, and Mao-Long Cai for collecting the specimens. Special thanks to Jun-Hao Huang for providing the information necessary for finding this species in the wild.

Author contributions

WXC and JXZ conceived and designed the study. YBL prepared the samples and conducted the sequencing. WXC, JW and MLM performed the bioinformatics analyses. WXC wrote the first draft of the manuscript. All authors reviewed and edited the manuscript and approved the final submission.

Funding

This work was supported by the National Natural Science Foundation of China, 32060306; and the National Parasitic Resources Center (CN), NPRC-2019-194-30.

Data availability

All data generated or analysed during this study are included in this published article, its supplementary information files and the NCBI's GenBank repository under the following accession numbers: PP543716 (chromosome 1) and PP543717 (chromosome 1). GenBank accession numbers of all mitogenomic sequences used in the analyses are available in Additional file 2.

Declarations

Ethics approval and consent to participate
All experiments were conducted on unprotected invertebrates, so no permits were required for the study. All methods are reported in accordance with ARRIVE guidelines for the reporting of animal experiments.

Consent for publication
Not applicable.

Competing interests
The authors declare no competing interests.

Received: 30 March 2024 / Accepted: 23 July 2024
Published online: 02 August 2024

References

1. Boore JL. Animal mitochondrial genomes. Nucleic Acids Res. 1999;27:1767–80.
2. Suga K, Mark Welch DB, Tanaka Y, Sakakura Y, Hagiwara A. Two circular chromosomes of unequal copy number make up the mitochondrial genome of the rotifer Brachionus plicatilis. Mol Biol Evol. 2008;25:1129–37.
3. Nie ZJ, Gu RB, Du FK, Shao NL, Xu P, Xu GC. Monogonont Rotifer, Brachionus calyciflorus, possesses exceptionally large, fragmented mitogenome. PLoS ONE. 2016;11:e0168263.
4. Mao M, Austin AD, Johnson NF, Dowton M. Coexistence of Minicircular and a highly rearranged mtDNA molecule suggests that recombination shapes mitochondrial Genome Organization. Mol Biol Evol. 2014;31:636–44.
5. Armstrong MR, Blok VC, Phillips MS. A multipartite mitochondrial genome in the potato cyst nematode Globodera Pallida. Genetics. 2000;154:181–92.
6. Phillips WS, Brown AMV, Howe DK, Peetz AB, Blok VC, Denver DR, et al. The mitochondrial genome of Globodera Ellingtonae is composed of two circles with segregated gene content and differential copy numbers. BMC Genomics. 2016;17:706.
7. Shao R, Kirkness EF, Barker SC. The single mitochondrial chromosome typical of animals has evolved into 18 minichromosomes in the human body louse, Pediculus humanus. Genome Res. 2009;19:904–12.
8. Shao R, Zhu X-Q, Barker SC, Herd K. Evolution of extensively fragmented mitochondrial genomes in the lice of humans. Genome Biol Evol. 2012;4:1088–101.
9. Rand DM. Why genomes in pieces? Revisited: sucking lice do their own thing in mtDNA circle game. Genome Res. 2009;19:700–2.
10. Xiong H, Barker SC, Burger TD, Raoult D, Shao R. Heteroplasmy in the Mitochondrial Genomes of Human Lice and ticks revealed by high throughput sequencing. PLoS ONE. 2013;8.
11. Feng S, Pozzi A, Stejskal V, Opit G, Yang Q, Shao R, et al. Fragmentation in mitochondrial genomes in relation to elevated sequence divergence and extreme rearrangements. BMC Biol. 2022;20:7.
12. Lynch M, Koskella B, Schaack S. Mutation pressure and the evolution of organelle genomic architecture. Science. 2006;311:1727–30.
13. Shtolz N, Mishmar D. The metazoan landscape of mitochondrial DNA gene order and content is shaped by selection and affects mitochondrial transcription. Commun Biol. 2023;6:1–15.
14. Jakovlić I, Zou H, Ye T, Wang G, Li W, Zhang D. Drivers of interlineage variability in mitogenomic evolutionary rates in flatworms (Platyhelminthes) are multifactorial. bioRxiv. 2022;2022.09.11.507443.
15. Zou H, Jakovlić I, Zhang D, Hua C-J, Chen R, Li W-X, et al. Architectural instability, inverted skews and mitochondrial phylogenomics of Isopoda: outgroup choice affects the long-branch attraction artefacts. R Soc Open Sci. 2020;7:191887.
16. Tan MH, Gan HM, Lee YP, Bracken-Grissom H, Chan T-Y, Miller AD, et al. Comparative mitogenomics of the Decapoda reveals evolutionary heterogeneity in architecture and composition. Sci Rep. 2019;9:1–16.
17. Jakovlić I, Zou H, Zhao X-M, Zhang J, Wang G-T, Zhang D. Evolutionary history of inversions in directional mutational pressures in crustacean mitochondrial genomes: implications for evolutionary studies. Mol Phylogenet Evol. 2021;164:107288.
18. Doublet V, Raimond R, Grandjean F, Lafitte A, Souty-Grosset C, Marcadé I, et al. Widespread atypical mitochondrial DNA structure in isopods (Crustacea, Peracarida) related to a constitutive heteroplasmy in terrestrial species. Genome. 2012;55:234–44.
19. Doublet V, Helleu Q, Raimond R, Souty-Grosset C, Marcadé I. Inverted repeats and genome architecture conversions of terrestrial isopods mitochondrial DNA. J Mol Evol. 2013;77:107–18.
20. Williams EP, Feng X, Place AR. Extensive heteroplasmy and evidence for Fragmentation in the Callinectes sapidus mitochondrial genome. J Shellfish Res. 2017;36:263–72.
21. Yeo DCJ, Ng PKL, Cumberlidge N, Magalhães C, Daniels SR, Campos MR. Global diversity of crabs (Crustacea: Decapoda: Brachyura) in freshwater. In: Balian EV, Lévêque C, Segers H, Martens K, editors. Freshwater Animal Diversity Assessment. Dordrecht: Springer Netherlands; 2008. pp. 275–86.
22. Cumberlidge N, Ng PKL, Yeo DCJ, Naruse T, Meyer KS, Esser LJ. Diversity, endemism and conservation of the freshwater crabs of China (Brachyura: Potamidae and Gecarcinucidae). Integr Zool. 2011;6:45–55.
23. Zhou X, Zhu C, Naruse T. Bottapotamon Nanan, a new species of freshwater crab (Decapoda, Brachyura, Potamidae) from Fujian Province, China. Crustaceana. 2008;81:1389–96.
24. Gao N, Cui Y-Y, Wang S-B, Zou J-X. Two new species and the molecular phylogeography of the freshwater crab genus Bottapotamon (Crustacea: Decapoda: Brachyura: Potamidae). PeerJ. 2019;7:e7980.
25. Zhang Z, Xing Y, Cheng J, Pan D, Lv L, Cumberlidge N, et al. Phylogenetic implications of mitogenome rearrangements in east Asian potamiscine freshwater crabs (Brachyura: Potamidae). Mol Phylogenet Evol. 2020;143:106669.
26. Ji Y-T, Zhou X-J, Yang Q, Lu Y-B, Wang J, Zou J-X. Adaptive evolution characteristics of mitochondrial genomes in genus Aparapotamon (Brachyura, Potamidae) of freshwater crabs. BMC Genomics. 2023;24:193.
27. Altschul SF, Madden TL, Schäffer AA, Zhang J, Zhang Z, Miller W, et al. Gapped BLAST and PSI-BLAST: a new generation of protein database search programs. Nucleic Acids Res. 1997;25:3389–402.
28. Burland TG. DNASTAR's lasergene sequence analysis software. In: Misener S, Krawetz SA, editors. Methods in Molecular Biology™. Totowa, NJ: Humana; 2000. pp. 71–91.
29. Bernt M, Donath A, Jühling F, Externbrink F, Florentz C, Fritzsch G, et al. MITOS: Improved de novo metazoan mitochondrial genome annotation. Mol Phylogenet Evol. 2013;69:313–9.
30. Laslett D, Canbäck B. ARWEN: a program to detect tRNA genes in metazoan mitochondrial nucleotide sequences. Bioinformatics. 2008;24:172–5.
31. Zhang D, Gao F, Jakovlić I, Zou H, Zhang J, Li WX, et al. PhyloSuite: an integrated and scalable desktop platform for streamlined molecular sequence data management and evolutionary phylogenetics studies. Mol Ecol Resour. 2020;20:348–55.
32. Minh BQ, Schmidt HA, Chernomor O, Schrempf D, Woodhams MD, von Haeseler A, et al. IQ-TREE 2: New models and efficient methods for phylogenetic inference in the genomic era. Mol Biol Evol. 2020;37:1530–4.
33. Foster PG. Modeling compositional heterogeneity. Syst Biol. 2004;53:485–95.
34. Zhang D, Zou H, Hua C-J, Li W-X, Mahboob S, Al-Ghanim KA, et al. Mitochondrial Architecture rearrangements produce asymmetrical nonadaptive mutational pressures that subvert the phylogenetic Reconstruction in Isopoda. Genome Biol Evol. 2019;11:1797–812.
35. Katoh K, Standley DM. MAFFT multiple sequence alignment software version 7: improvements in performance and usability. Mol Biol Evol. 2013;30:772–80.
36. Kalyaanamoorthy S, Minh BQ, Wong TKF, Von Haeseler A, Jermiin LS. ModelFinder: fast model selection for accurate phylogenetic estimates. Nat Methods. 2017;14:587–9.
37. Ronquist F, Teslenko M, Van Der Mark P, Ayres DL, Darling A, Höhna S, et al. Mrbayes 3.2: efficient bayesian phylogenetic inference and model choice across a large model space. Syst Biol. 2012;61:539–42.
38. Minh BQ, Nguyen MAT, von Haeseler A. Ultrafast approximation for Phylogenetic Bootstrap. Mol Biol Evol. 2013;30:1188–95.
39. Tsang LM, Schubart CD, Ahyong ST, Lai JCY, Au EYC, Chan T-Y, et al. Evolutionary history of true crabs (Crustacea: Decapoda: Brachyura) and the origin of Freshwater Crabs. Mol Biol Evol. 2014;31:1173–87.
40. Pang X, Han C, Guo B, Liu K, Lin X, Lu X. The first complete mitochondrial genome of Eucrate crenata (Decapoda: Brachyura: Goneplacidae) and phylogenetic relationships within Infraorder Brachyura. Genes. 2022;13:1127.
41. Xiang C, Gao F, Jakovlić I, Lei H, Hu Y, Zhang H, et al. Using PhyloSuite for molecular phylogeny and tree-based analyses. iMeta. 2023;2:e87.
42. Struck TH. TreSpEx—Detection of Misleading Signal in phylogenetic reconstructions based on Tree Information. Evol Bioinforma Online. 2014;10:51–67.
43. Okonechnikov K, Golosova O, Fursov M. The UGENE team. Unipro UGENE: a unified bioinformatics toolkit. Bioinformatics. 2012;28:1166–7.

44. Lorenz R, Bernhart SH, Höner zu Siederdissen C, Tafer H, Flamm C, Stadler PF, et al. ViennaRNA Package 2 0 Algorithms Mol Biol. 2011;6:26.
45. Benson G. Tandem repeats finder: a program to analyze DNA sequences. Nucleic Acids Res. 1999;27:573–80.
46. Greiner S, Lehwark P, Bock R. OrganellarGenomeDRAW (OGDRAW) version 1.3.1: expanded toolkit for the graphical visualization of organellar genomes. Nucleic Acids Res. 2019;47:W59–64.
47. Wertheim JO, Murrell B, Smith MD, Kosakovsky Pond SL, Scheffler K. RELAX: detecting relaxed selection in a phylogenetic Framework. Mol Biol Evol. 2015;32:820–32.
48. Bzymek M, Lovett ST. Instability of repetitive DNA sequences: the role of replication in multiple mechanisms. Proc Natl Acad Sci. 2001;98:8319–25.
49. Castellana S, Vicario S, Saccone C. Evolutionary patterns of the mitochondrial genome in Metazoa: exploring the role of mutation and selection in mitochondrial protein–coding genes. Genome Biol Evol. 2011;3:1067–79.
50. Pan D, Shi B, Du S, Gu T, Wang R, Xing Y, et al. Mitogenome phylogeny reveals Indochina Peninsula origin and spatiotemporal diversification of freshwater crabs (Potamidae: Potamiscinae) in China. Cladistics. 2021;38:1–12.
51. Wang Y-F, Yang Q, Xu S-X, Zhao M-J, Zou J-X. The complete mitochondrial genome of the freshwater crab Bottapotamon lingchuanense Türkay and Dai 1997 (Decapoda: Brachyura: Potamoidea). Mitochondrial DNA Part B Resour. 2021;6:1554–6.
52. Lan Y, Sun J, Bartlett DH, Rouse GW, Tabata HG, Qian P-Y. The deepest mitochondrial genome sequenced from Mariana Trench Hirondellea gigas (Amphipoda). Mitochondrial DNA Part B. 2016;1:802–3.
53. Gan HM, Grandjean F, Jenkins TL, Austin CM. Absence of evidence is not evidence of absence: Nanopore sequencing and complete assembly of the European lobster (Homarus gammarus) mitogenome uncovers the missing nad2 and a new major gene cluster duplication. BMC Genomics. 2019;20:335.
54. Hommelsheim CM, Frantzeskakis L, Huang M, Ülker B. PCR amplification of repetitive DNA: a limitation to genome editing technologies and many other applications. Sci Rep. 2014;4:5052.
55. Sweet AD, Johnson KP, Cameron SL. Independent evolution of highly variable, fragmented mitogenomes of parasitic lice. Commun Biol. 2022;5:1–10.
56. Hazkani-Covo E, Zeller RM, Martin W. Molecular poltergeists: mitochondrial DNA copies (numts) in sequenced nuclear genomes. PLoS Genet. 2010;6:e1000834.
57. Zhang D, Jakovlić I, Zou H, Liu F, Xiang C-Y, Gusang Q, et al. Strong mitonuclear discordance in the phylogeny of Neodermata and evolutionary rates of Polyopisthocotylea. Int J Parasitol. 2024;54:213–23.
58. Gissi C, Iannelli F, Pesole G. Evolution of the mitochondrial genome of Metazoa as exemplified by comparison of congeneric species. Heredity. 2008;101:301–20.
59. Azevedo JLB, Hyman BC. Molecular characterization of lengthy mitochondrial DNA duplications from the parasitic nematode Romanomermis Culicivorax. Genetics. 1993;133:933–42.
60. Zou H, Jakovlić I, Chen R, Zhang D, Zhang J, Li W-X, et al. The complete mitochondrial genome of parasitic nematode Camallanus cotti: extreme discontinuity in the rate of mitogenomic architecture evolution within the Chromadorea class. BMC Genomics. 2017;18:840.
61. Beckenbach AT. Mitochondrial genome sequences of representatives of three families of scorpionflies (Order Mecoptera) and evolution in a major duplication of coding sequence. Genome. 2011;54:368–76.
62. Fujita MK, Boore JL, Moritz C. Multiple origins and Rapid Evolution of duplicated mitochondrial genes in parthenogenetic geckos (Heteronotia binoei; Squamata, Gekkonidae). Mol Biol Evol. 2007;24:2775–86.
63. Mueller RL, Boore JL. Molecular mechanisms of extensive mitochondrial gene rearrangement in Plethodontid Salamanders. Mol Biol Evol. 2005;22:2104–12.
64. Levinson G, Gutman G. a. Slipped-strand mispairing: a major mechanism for DNA sequence evolution. Mol Biol Evol. 1987;4:203–21.
65. Shao R, Li H, Barker SC, Song S. The mitochondrial genome of the Guanaco Louse, Microthoracius praelongiceps: insights into the ancestral mitochondrial karyotype of sucking lice (Anoplura, Insecta). Genome Biol Evol. 2017;9:431–45.
66. Sammler S, Ketmaier V, Havenstein K, Tiedemann R. Intraspecific rearrangement of duplicated mitochondrial control regions in the Luzon Tarictic Hornbill Penelopides manillae (Aves: Bucerotidae). J Mol Evol. 2013;77:199–205.
67. San Mauro D, Gower DJ, Zardoya R, Wilkinson M. A hotspot of gene order rearrangement by tandem duplication and random loss in the vertebrate mitochondrial genome. Mol Biol Evol. 2006;23:227–34.
68. Mindell DP, Sorenson MD, Dimcheff DE. Multiple independent origins of mitochondrial gene order in birds. Proc Natl Acad Sci U S A. 1998;95:10693–7.
69. Dowton M, Austin AD. Evolutionary dynamics of a mitochondrial rearrangement 'Hot spot' in the Hymenoptera. Mol Biol Evol. 1999;16:298–309.
70. Dowton M, Cameron SL, Dowavic JI, Austin AD, Whiting MF. Characterization of 67 mitochondrial tRNA gene rearrangements in the Hymenoptera suggests that mitochondrial tRNA gene position is selectively neutral. Mol Biol Evol. 2009;26:1607–17.
71. Bernt M, Bleidorn C, Braband A, Dambach J, Donath A, Fritzsch G, et al. A comprehensive analysis of bilaterian mitochondrial genomes and phylogeny. Mol Phylogenet Evol. 2013;69:352–64.
72. Struck TH, Golombek A, Hoesel C, Dimitrov D, Elgetany AH. Mitochondrial genome evolution in Annelida—A systematic study on conservative and variable gene orders and the factors influencing its evolution. Syst Biol. 2023;72:925–45.
73. Zou H, Lei H-P, Chen R, Chen F-L, Li W-X, Li M, et al. Evolutionary rates of mitochondrial sequences and gene orders in Spirurina (Nematoda) are episodic but synchronised. Water Biol Secur. 2022;1:100033.
74. Bauzà-Ribot MM, Juan C, Nardi F, Oromí P, Pons J, Jaume D. Mitogenomic Phylogenetic Analysis Supports Continental-Scale Vicariance in Subterranean Thalassoid crustaceans. Curr Biol. 2012;22:2069–74.
75. Najer T, Doña J, Buček A, Sweet AD, Sychra O, Johnson KP. Mitochondrial genome fragmentation is correlated with increased rates of molecular evolution. PLOS Genet. 2024;20:e1011266.
76. Shao R, Dowton M, Murrell A, Barker SC. Rates of Gene Rearrangement and Nucleotide Substitution are correlated in the mitochondrial genomes of insects. Mol Biol Evol. 2003;20:1612–9.
77. Hassanin A. Phylogeny of Arthropoda inferred from mitochondrial sequences: strategies for limiting the misleading effects of multiple changes in pattern and rates of substitution. Mol Phylogenet Evol. 2006;38:100–16.
78. Xu W, Jameson D, Tang B, Higgs PG. The relationship between the rate of molecular evolution and the rate of genome rearrangement in animal mitochondrial genomes. J Mol Evol. 2006;63:375–92.
79. Chong RA, Mueller RL. Evolution along the mutation gradient in the dynamic mitochondrial genome of salamanders. Genome Biol Evol. 2013;5:1652–60.
80. Lagisz M, Poulin R, Nakagawa S. You are where you live: parasitic nematode mitochondrial genome size is associated with the thermal environment generated by hosts. J Evol Biol. 2013;26:683–90.
81. Zou H, Chen F-L, Li W-X, Li M, Lei H-P, Zhang D, et al. Inverted base composition skews and discontinuous mitochondrial genome architecture evolution in the Enoplea (Nematoda). BMC Genomics. 2022;23:376.
82. Jakovlić I, Zou H, Chen J-H, Lei H-P, Wang G-T, Liu J, et al. Slow crabs - fast genomes: locomotory capacity predicts skew magnitude in crustacean mitogenomes. Mol Ecol. 2021;30:5488–502.
83. Reyes A, Gissi C, Pesole G, Saccone C. Asymmetrical directional mutation pressure in the mitochondrial genome of mammals. Mol Biol Evol. 1998;15:957–66.
84. Oliveira MT, Haukka J, Kaguni LS. Evolution of the Metazoan mitochondrial replicase. Genome Biol Evol. 2015;7:943–59.
85. Rand DM. Endotherms, ectotherms, and mitochondrial genome-size variation. J Mol Evol. 1993;37:281–95.
86. Jakovlić I, Zou H, Ye T, Zhang H, Liu X, Xiang C-Y, et al. Mitogenomic evolutionary rates in Bilateria are influenced by parasitic lifestyle and locomotory capacity. Nat Commun. 2023;14:6307.
87. Sun Y-B, Shen Y-Y, Irwin DM, Zhang Y-P. Evaluating the roles of energetic functional constraints on Teleost mitochondrial-encoded protein evolution. Mol Biol Evol. 2011;28:39–44.

Publisher's Note